Available online at www.sciencedirect.com
SCIENCE DIRECT®
Journal of Power Sources 142 (2005) 253–263
JOURNAL OF POWER SOURCES
www.elsevier.com/locate/jpowsour

Real-time strategy for active power sharing in a fuel cell powered battery charger

Zhenhua Jiang*, Roger A. Dougal

Department of Electrical Engineering, University of South Carolina, Columbia, SC 29208, USA

Received 30 September 2004; accepted 25 October 2004
Available online 19 December 2004

Abstract

This paper presents a real-time strategy for active power sharing in a fuel cell powered battery charging station. This control scheme can adjust the charging currents of the batteries being simultaneously charged in real-time according to the estimated state-of-charge (SOC) which is obtained by estimating the battery open-circuit voltage with current correction and linearly fitting between the open-circuit voltage and the state-of-charge. The charge controller that executes the real-time strategy is designed and implemented in Matlab/Simulink for both system simulation and experimental tests. Simulation results show that all batteries can become fully charged simultaneously with the real-time strategy and the estimation method for battery state-of-charge is effective for the active power sharing strategy. Experiment results validate the simulation and show that the battery state-of-charge estimation method is practical.

Keywords: Fuel cell; Battery charger; Active power sharing; Control strategy; Real-time; Power converter

1. Introduction

The limited usable time of rechargeable batteries, which are playing an increasingly significant role in the utilization of portable electronic devices such as portable computers, cellular phones and camcorders [1], makes it essential to develop some kind of portable battery charging system. The fuel cell, which is emerging as one of the most promising technologies for the future power sources [2,3], may provide a good solution for powering the portable charging station [4], which may be far away from the utility power. However, when charging advanced technology batteries such as lithium ion cells, it is hazardous to exceed certain current or voltage limits. The fuel cell has a limited power capacity, and large power demand may go beyond its power limit. Both the fuel cell and lithium ion battery are strongly nonlinear [5–8]. All of these present some difficulty for the control design.

In order to meet the simultaneous requirements of multiple users, power converters are connected in parallel, each for one battery pack. In the general case, the initial states of the batteries being inserted are considerably different. A battery with lower initial state-of-charge (SOC) may require a larger charging current or otherwise a longer charging time. Therefore, the power from the fuel cell should be distributed efficiently among the charging branches. Three basic static control schemes have been initially investigated in [4]. Among these three strategies, with equal rate charging strategy, the battery with the highest initial state-of-charge can become full fastest but the total charging time is the longest due to the most depleted battery. Proportional rate charging strategy and pulse current charging strategy change the situation and it is possible for all the batteries to become fully charged almost simultaneously. However, with these static strategies, the charging currents or the duty cycles of the pulse currents are set up at the very beginning according to the estimation of the initial states and do not change any more during the current regulation mode. The simultaneous termination of charging is not guaranteed. In order to reduce

* Corresponding author. Tel.: +1 803 777 9314; fax: +1 803 777 8045.
E-mail address: jiang@engr.sc.edu (Z. Jiang).

0378-7753/$ – see front matter © 2004 Elsevier B.V. All rights reserved.
doi:10.1016/j.jpowsour.2004.10.025

Nomenclature

a, b, c	constants used in Eq. (7)
C	charge remaining in the battery (A h or C)
C_0	rated capacity of the battery (A h or C)
d	duty cycle in the current time step
d_i	duty cycle of the ith buck converter
d_{old}	duty cycle in the previous time step
I	sampled charging current of the battery (A)
I_{fc}	current available from the fuel cell (A)
I_i	charging current of the ith battery (A)
I_{lim}	preset limit for the total charging current (A)
I_{ref}	reference charging current of the battery (A)
$k_{\text{i}i}$	integral gain for current regulation
$k_{\text{i}v}$	integral gain for voltage regulation
$k_{\text{p}i}$	proportional gain for current regulation
$k_{\text{p}v}$	proportional gain for voltage regulation
P_{fc}	power available from the fuel cell (W)
P_i	power to the ith charging channel (W)
r	equivalent series resistance (ESR) of the battery
SOC_i	state-of-charge of the ith battery
SOC_0	initial state-of-charge
t_{end}	total charging time (h)
V	sampled charging voltage of the battery (V)
V_{ref}	reference charging voltage of the battery (V)
v_1	up-limit voltage corresponding with the condition that the state-of-charge is approximately equal to 0.9 (V)
v_2	low-limit voltage corresponding with the condition that the state-of-charge is approximately equal to 0.1 (V)

the total charging time and the fuel use, the power sharing among the battery banks should be optimized in real-time and vary with the state-of-charge of each battery.

The state-of-charge is a defined variable that is used to represent the charge remaining in the battery and it is widely used in the electrochemical field. However, it cannot be measured directly and it also is difficult to estimate the state-of-charge. Many people have studied the approaches to the state-of-charge estimation. Liu et al. [9] presented two methods to estimate the state-of-charge, whereas the ampere–hours method requires the information of initial state-of-charge and the recursive method needs many offline experimental data to obtain the many parameters. In this application, a simple and practical approach may be desired to estimate the state-of-charge based on the measured charging current and voltage of the battery.

This paper presents a novel real-time control strategy (RTCS) for active power sharing in a fuel cell powered battery charging station. The remainder of this paper is organized as follows. The system design and the control issues involved are discussed in Section 2. Section 3 addresses the real-time control strategy that can adjust the charging currents according to the estimated state-of-charge which is obtained by estimating the battery open-circuit voltage with current correction and linearly fitting between the open-circuit voltage and state-of-charge. Section 4 presents the Simulink implementation of the charging controller. The simulation results are given in Section 5. Section 6 demonstrates the experiment results and validates the control strategy. Conclusions are made in Section 7.

2. System design and problem definition

In general, the battery charging station should allow multiple batteries to be charged simultaneously, and it should be possible to insert or retrieve any battery at any time. A typical case of three charging channels is studied in this paper, which can represent the general solution of many charging channels.

The block diagram of the fuel cell powered battery charging station is shown in Fig. 1, where the parameters are also shown. A fuel cell stack, which is the power generation system, is used to charge up to three lithium ion battery packs, each through a DC/DC step-down buck converter. Each battery contains four series-connected cells. The buck converters control the charging current and voltage supplied to each battery, and allocate the available power among the batteries. A controller is used to coordinate these power converters. The real-time control strategy for active power sharing in this fuel cell/battery system is implemented in this controller. The charging currents and battery voltages are monitored and fed to the controller. This controller can calculate the reference charging current for each channel and the corresponding

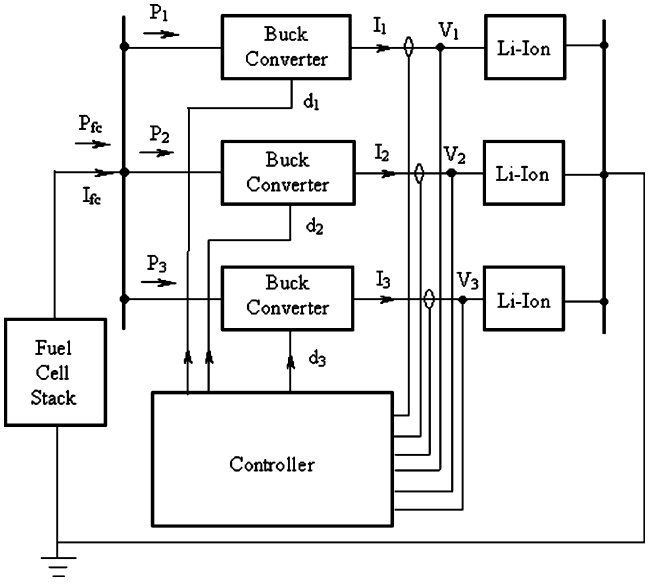

Fig. 1. Block diagram and parameter definition of the fuel-cell-powered battery-charging station.

duty cycle. It can also output the PWM switching waves to the drivers of the switches in buck converters.

As shown in Fig. 1, three-buck converters are connected in parallel to a single fuel cell power source. The active power available from the fuel cell is distributed among the three batteries according to (1).

$$P_{\text{fc}} = P_1 + P_2 + P_3 \tag{1}$$

where P_1, P_2, and P_3 are the power to three charging channels, respectively, and P_{fc} is the power from the fuel cell.

In practice, the power distribution among the batteries is realized by regulating the charging currents of the batteries. The following equation relates the current from the fuel cell to three charging currents, assuming no power loss in these power converters.

$$I_{\text{fc}} = d_1 I_1 + d_2 I_2 + d_3 I_3 \tag{2}$$

where I_1, I_2, and I_3, respectively, are the currents to three batteries, I_{fc} the current from the fuel cell, and d_1, d_2, and d_3 are the duty cycles of three-buck converters, respectively, and have values between 0 and 1.

Since the power from the fuel cell is limited, it is desirable that the fuel cell operates at the maximum power point. Therefore, the sum of the right hand side in (2) should be less than the current available from the fuel cell corresponding to the maximum power point. Considering that the variations in the voltages of the fuel cell and batteries are not too large, the duty cycle will vary within a limited small range, for example, between 0.7 and 0.75. Based on this, we can take the following expression as a criterion for power distribution among the batteries.

$$I_1 + I_2 + I_3 \leq I_{\text{lim}} \tag{3}$$

where I_{lim} is a preset limit for the total charging current that can be estimated according to the current available from the fuel cell corresponding to the maximum power point and the average duty cycle of power converters.

Eq. (3) gives a basic requirement for design of active power sharing strategy. Actually, the goal of the real-time control strategy is to utilize the power of the fuel cells efficiently and to distribute the power among batteries reasonably.

3. Real-time strategy for active power sharing

3.1. Real-time control strategy

The users may have different requirements for charging their batteries according to their own needs. Some people may require that the batteries be fully charged within the shortest period of time, while others may need a better life expectation for their batteries. This paper, aiming to discover an appropriate control scheme for minimizing the charging time, investigates a real-time control strategy for DC charging to coordinate the active power sharing. DC charging protocol can help to protect the battery from overcharging. Under this protocol, the battery is charged to an end potential using a direct current. The potential is then held constant after this potential is reached, and the charging current will taper gradually. The charging process terminates when the current reaches a preset small value during the constant voltage mode.

In order to discover the real-time control strategy, let's consider a basic relationship between the charge level of the battery and the charging current. The charge of the battery can be expressed as follows:

$$C(t_{\text{end}}) = C_0\,\text{SOC}_0 + \int_0^{t_{\text{end}}} I\,\text{d}t \tag{4}$$

where C_0 is the rated capacity of the battery (Ahr or C), SOC_0 the initial state-of-charge, I the charging current (A), t_{end} the total charging time (h). In (4), $C_0\,\text{SOC}_0$ stands for the initial charge in the battery. From (4), it is seen that the charge that the battery will need to get fully charged is the integral of the charging current over the total charging time until the battery is full. While the state-of-charge represents the charge level remaining in the battery, the depth of discharge indicates the charge needed to fill the battery. It is calculated as unity minus state-of-charge. A basic strategy reported in [4], called equal-rate charging, is to use direct currents of the same magnitude to charge different batteries. The charging time will be approximately proportional to the depth of discharge (neglecting nonlinearity). On the other hand, if we want all the batteries to become fully charged during the same period of time, the charging current of each battery can be proportional to its fraction of the total depth of discharge. Therefore, the charging current for each battery can be calculated according to (5)

$$I_i = I_{\text{lim}} \cdot \frac{1 - \text{SOC}_i}{\sum_{i=1}^{3}(1 - \text{SOC}_i)}, \quad i = 1, 2, 3 \tag{5}$$

where I_i is the charging current of the ith battery, I_{lim} the total available charging current, and SOC_i is the state-of-charge of the ith battery. It is clear that the current sharing strategy shown in (5) meets the criterion given in (3) and utilizes as much power of the fuel cell as possible. The difference between this strategy and proportional rate charging strategy reported in [5] is that the real-time control strategy can adjust the charging currents in real-time according to the estimated state-of-charge of each battery while proportional rate charging strategy just determines the charging currents of the batteries at the beginning according to the estimates of the initial battery state-of-charge.

The detail of the algorithm that implements this real-time charging strategy is explained as follows. In this algorithm, I_{lim} is the limit of total charging current. V_{ref} is battery end potential, which is usually 4.2 V for each cell. I_1, I_2, I_3 are the charging currents of three batteries, respectively. (Here we assume that the maximum current available from the fuel cell, I_{lim}, is less than the sum of the maximum safe charging currents for all of the batteries.)

- $I_{\text{ref},i} = I_{\text{lim}} \times (1 - \text{SOC}_i)/[(1 - \text{SOC}_1) + (1 - \text{SOC}_2) + (1 - \text{SOC}_3)]$, $i = 1, 2, 3$.
- If $V_1 = V_{\text{ref}}$, I_1 is tapering.
- If $V_2 = V_{\text{ref}}$, I_2 is tapering.
- If $V_3 = V_{\text{ref}}$, I_3 is tapering.
- If $I_i < 0.1 \times I_{\text{ref},i}$, then $I_{\text{ref},i} = 0$, where $i = 1, 2, 3$.

3.2. Battery state-of-charge estimation

In the above control strategy, the charging currents vary with the state-of-charge of each battery. Since it is impossible to measure the state-of-charge directly, a method should be found to estimate the state-of-charge according to the measured battery voltage and charging current. For lithium-ion batteries, an approximately linear relationship between the state-of-charge and open-circuit voltage can be found when the state-of-charge is not within the extreme range, i.e., if the state-of-charge is between 0.1 and 0.9. Therefore, the state-of-charge can be estimated by measuring the battery voltage. In this paper, the state-of-charge is estimated according to a piecewise linear relationship, which is given in (7).

$$\text{SOC} = \begin{cases} 0.9, & v_o \geq v_1 \\ \frac{v_0 - a}{b} + c, & v_2 < v_o < v_1 \\ 0.1, & v_o \leq v_2 \end{cases} \quad (7)$$

where a, b and c are constants and they can be easily obtained from values v_1 and v_2, v_0 is the battery open-circuit voltage. This estimation of the battery state-of-charge is shown in Fig. 2 (see Line a). The measured voltage versus state-of-charge relation is represented by Curve 1. When the open-circuit voltage exceeds an up-limit (v_1) that corresponds with the condition that the state-of-charge is approximately equal to 0.9, the estimate is cut off to 0.9. In this case, the battery-charging station is usually working under constant voltage mode and the battery voltage does not change. The charging current is not determined by the charging controller itself, but by the internal potential and terminal voltage of the battery. It is not necessary to estimate the state-of-charge since the information about state-of-charge is useful only when the charger works under current regulation mode. When the open-circuit voltage is below a down-limit (v_2) that corresponds with the condition that the state-of-charge is approximately equal to 0.1, the estimate is cut off to 0.1. In this case, the estimated value for depth-of-discharge is 0.9, and the fraction of the depth-of-discharge is very close to that using a more accurate value of the state-of-charge. This approximation does not affect the performance of the algorithm significantly, as will be shown later in simulation and experiment. When the open-circuit voltage falls between v_1 and v_2, the estimate of the state-of-charge is a linear function of the battery open-circuit voltage.

The values v_1 and v_2 corresponding to the state-of-charge values between 0.9 and 0.1, respectively, can be obtained by measuring the open-circuit voltage when charging the battery to 90% and 10% charge levels. The state-of-charge of the battery is decided using the following approach. Each battery is discharged to full depletion. A constant current is then applied to charge the battery until it is full and the total charging time is recorded. After fully depleting this battery, charging this battery with the same current for a proportion (equal to the state-of-charge in magnitude) of the total charging time can obtain a desired state-of- charge.

For lithium-ion batteries from different manufactures, the voltage versus state-of-charge curves may be slightly different (for example, see Curve 2 in Fig. 2). It is possible to obtain a series of parameters for different batteries from some major manufactures through the same set of experiments. These parameters can be preset in the controller. When the users select their battery type, the corresponding parameter set will be used for the estimation of the state-of-charge.

In the above estimation, the choice of the range of linear fitting is somehow arbitrary. This choice will affect the error between the estimated and actual state-of-charge. For Curve 2 in Fig. 2, if state-of-charge range of the linear fitting is between 0.2 and 0.8, the estimate of state-of-charge will be closer to the actual value when the state-of-charge of the battery is within this range. However, there will be larger discrepancy between the estimated and actual state-of-charge when the actual state-of-charge is beyond this range. There

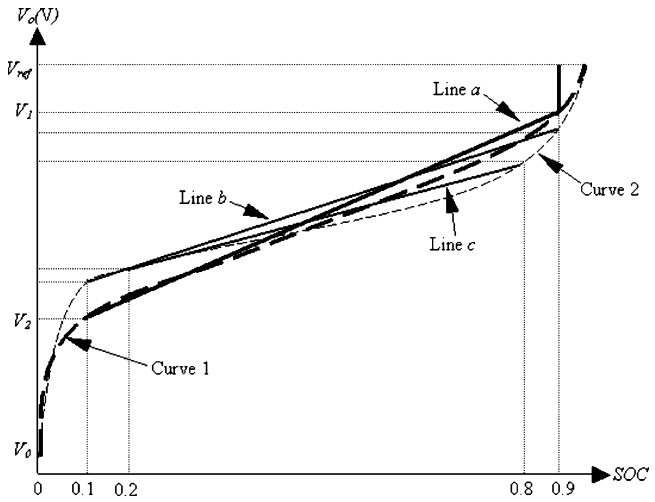

Fig. 2. Linear fitting between the open-circuit voltage and the state-of-charge of the battery.

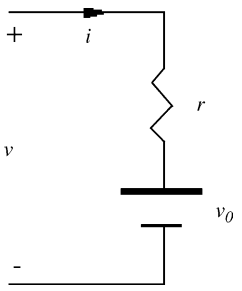

Fig. 3. Illustration of the equivalent circuit for estimation of the open-circuit voltage of the battery.

exists a tradeoff for the linear fitting range, depending on the general battery charge level.

While this approach to estimating the battery state-of-charge is applicable to static charging strategies, with real-time charging strategy, it is impossible to directly measure the open-circuit voltage when the battery is being charged. Nevertheless, when a voltage is applied to charge the battery, the internal potential of the battery is equal to the terminal voltage when the battery is open, which does not change with the external voltage being imposed across it at this moment. The equivalent circuit of the battery when a charging voltage is applied to the battery is illustrated in Fig. 3.

From Fig. 3, it is clear that the battery open-circuit voltage v_0 can be estimated from the following equation:

$$v_0 = v - ir \tag{8}$$

where v and i are the measured battery voltage and charging current, respectively, r the equivalent series resistance (ESR) of the battery. This current correction term is important to the state-of-charge estimate when the initial conditions of the batteries are widely disparate.

The proposed method for state-of-charge estimation is very simple and easily realized. Essentially, we need only to estimate the state-of-charge in order to decide how to divide the available current between the batteries. The actual state-of-charge is not of interest to this current distribution strategy, although it is useful in determining when the charging process terminates. If the estimate differs from actual state-of-charge, it only means that it takes slightly longer to charge the system of batteries because some battery gets less than its fair share of the current. As will be shown later, this estimate is effective for the active power sharing strategy.

4. Simulink implementation of charge controller

Mathworks' Matlab/Simulink was selected as the tool for the control system design for two reasons. First, an interface to Matlab/Simulink is available in the VTB environment, which makes it possible to test the control algorithm with

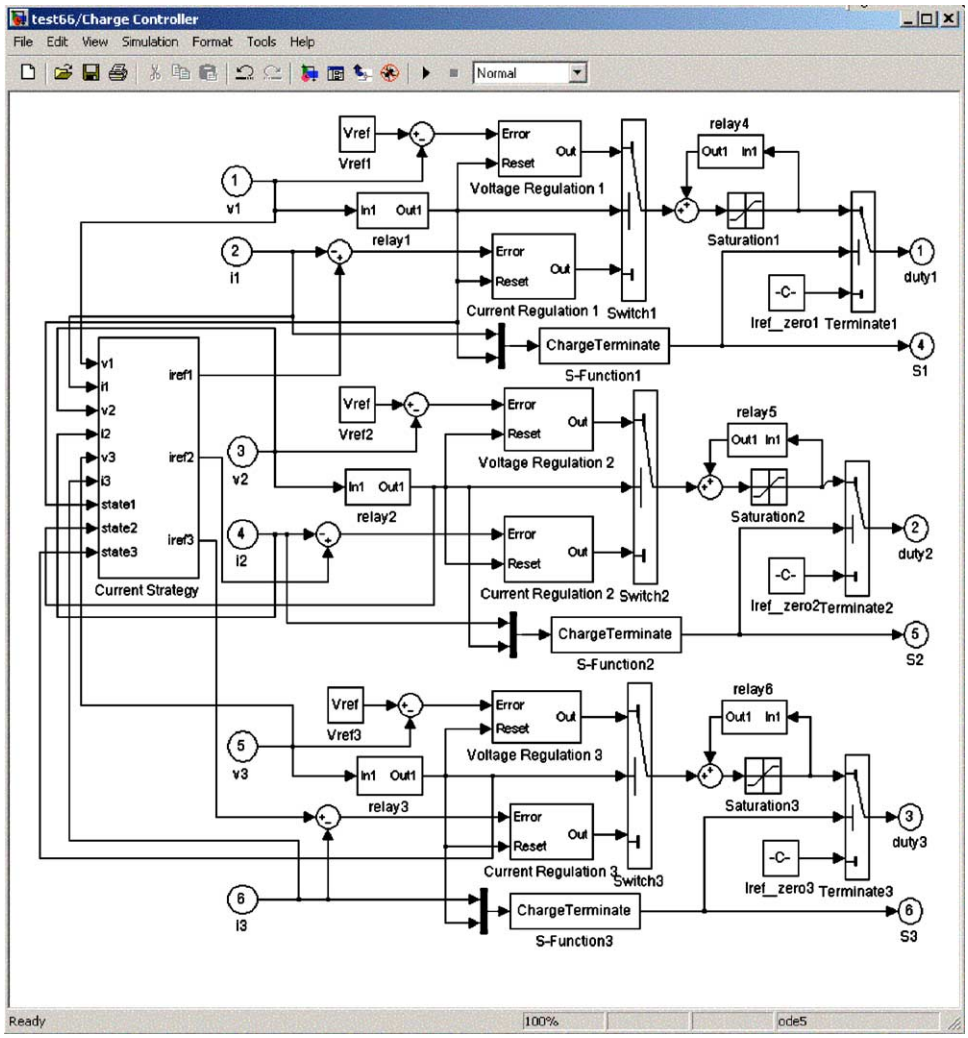

Fig. 4. Simulink model of the proposed battery charge controller for DC charging.

very detailed models of all of the hardware components, including fuel cell, batteries, and power electronics. Secondly, the Matlab software provides an interface layer to dSPACE hardware. The experimental validation can be performed by compiling Simulink codes of the controller and downloading onto the dSPACE platform to control the real hardware.

The Simulink model of the charge controller that implements the real-time charging strategy is shown in Fig. 4. The main functional blocks in the model are the charging current strategy module, current regulation module, voltage regulation module, and charging termination decision module.

The charging current strategy module is to calculate the reference charging currents according to the measured battery voltages and currents and it is developed based on the proposed current (or active power) sharing algorithm which is shown in (5), (7) and (8). The Simulink implementation of this module is shown in Fig. 5. The total available charging current is calculated according to the regulation mode and the charging currents. The depth of discharge is estimated for each battery based on the measured voltage and current. Based on these, the reference charging current for each channel is obtained.

The current and voltage regulation modules in Fig. 4 are used to compute the duty cycles to the buck converters according to the reference currents from the charging current strategy module and the reference voltages, respectively. The proportional-integral approach is used to regulate the charging currents and voltages. The current and voltage regulations are formulated in (9) and (10), respectively.

$$d = d_{\text{old}} + k_{\text{pi}}(I_{\text{ref}} - I) + k_{\text{ii}} \int (I_{\text{ref}} - I)\,\mathrm{d}t \tag{9}$$

$$d = d_{\text{old}} + k_{\text{pv}}(V_{\text{ref}} - V) + k_{\text{iv}} \int (V_{\text{ref}} - V)\,\mathrm{d}t \tag{10}$$

where V, I are the sampled voltage and current of the battery, d and d_{old} the current and previous duty cycles used to control the buck converter, V_{ref} and I_{ref} the reference voltage and charging current of the battery, k_{pi}, k_{ii}, and k_{pv}, k_{iv} are proportional and integral gains for current and voltage, respectively.

The charging termination decision module in Fig. 4, implemented by an S-function, can determine when the charging process stops and output a signal to the corresponding power converter.

5. Simulation results

In order to investigate the performance of the proposed real-time control strategy, a simulation study was first conducted in the VTB [10], which is endowed with mechanisms for importing models from Matlab and co-simulating with Simulink. Fig. 6 shows the VTB schematic view of the sys-

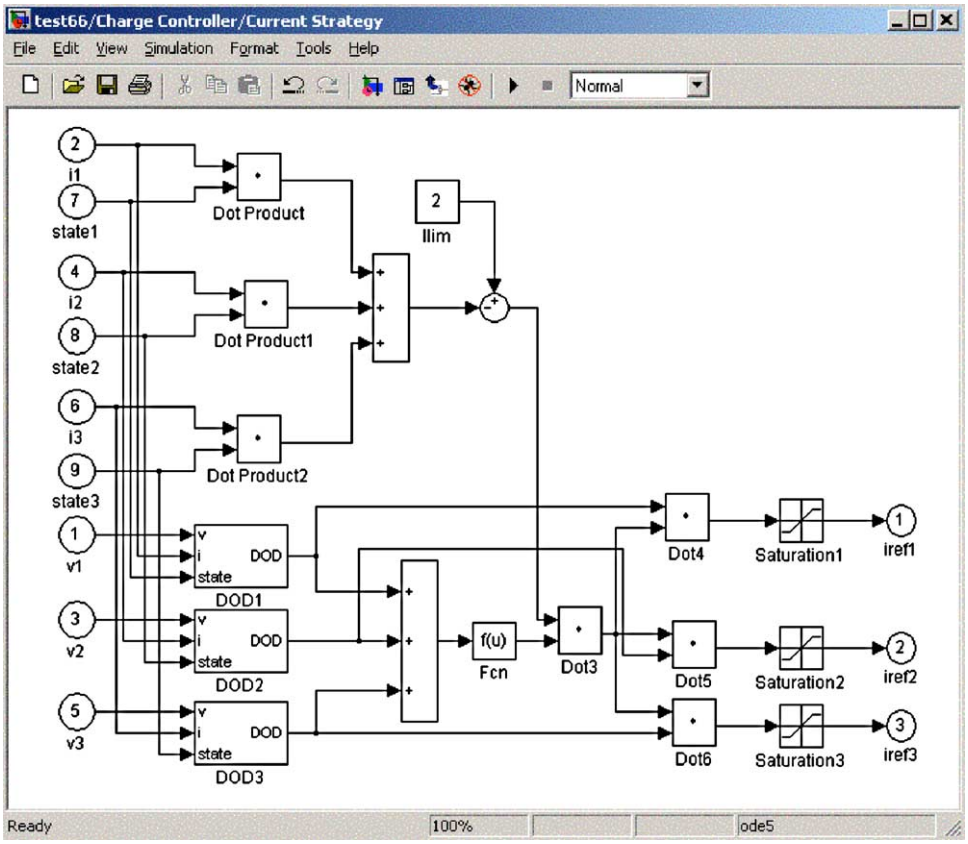

Fig. 5. Model for charging current strategy module.

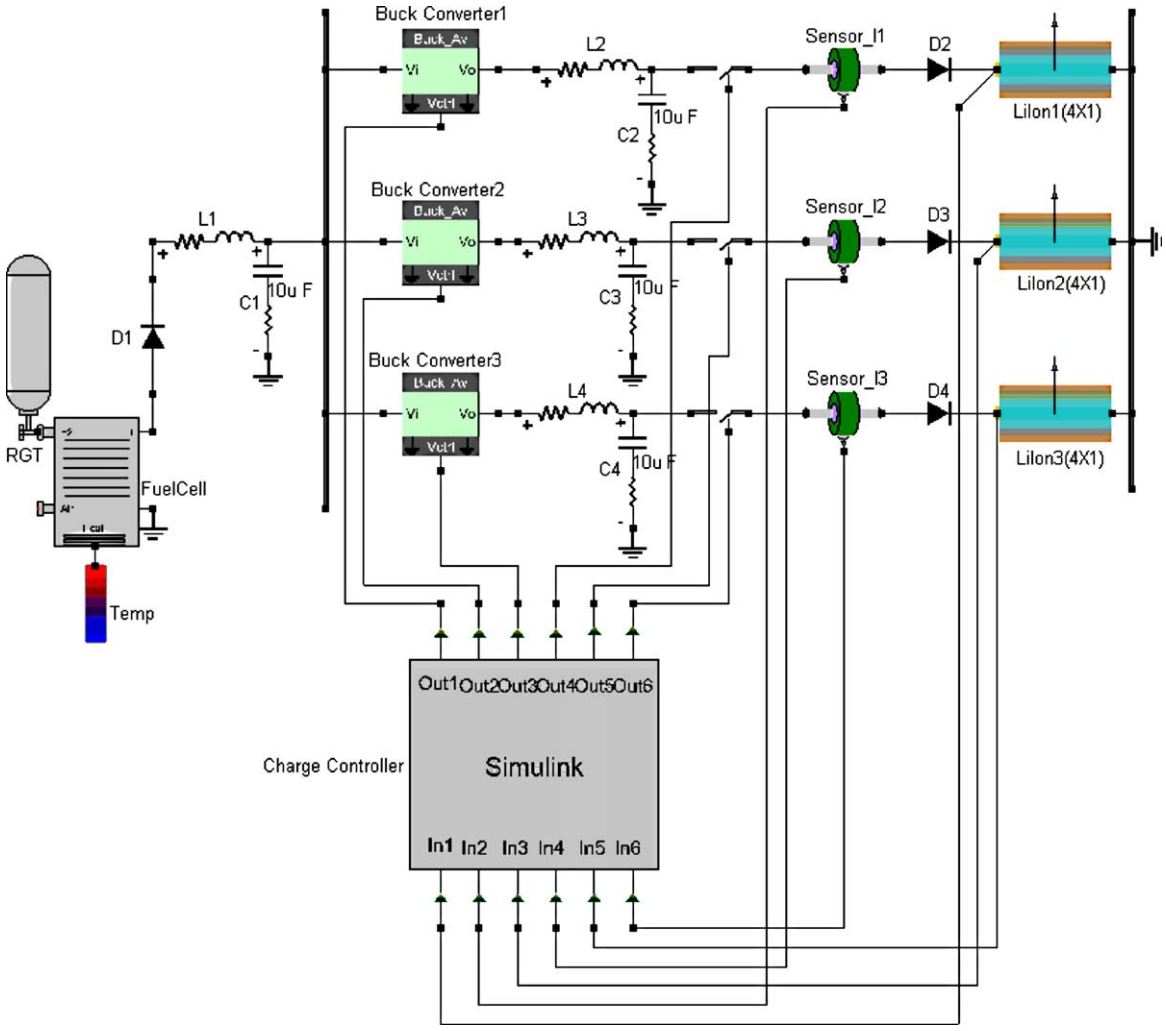

Fig. 6. VTB schematic view of the fuel-cell-powered battery-charging station.

tem shown in Fig. 1. The power source is a 25-cell PEM fuel cell stack. Each battery is a 4×1 (series by parallel connections) array of lithium ion cells. The capacity of each battery is 1500 mAh. The initial states of charge of the batteries are 0.6, 0.5, and 0.4, respectively. The total available charging current is 2 A. Each power converter is implemented by a switching-average buck converter model in series with a low pass filter. The controller is implemented in the Simulink model as shown in Fig. 4 and embedded to VTB simulation. The simulation was run for 2 h (7200 s), and the simulation results under the proposed real-time control strategy are shown in Fig. 7.

Fig. 7a and b show the voltages and charging currents of the batteries respectively. It is seen that the battery with the highest state-of-charge (thus the highest initial voltage) is charged at the lowest current. The charging currents vary with the estimate of state-of-charge. There is some difference between estimated and accurate state-of-charge, which can be seen from Fig. 7c. This is because the accurate state-of-charge is related to the nonlinear physics inside the battery while the estimate of state-of-charge is based on a linear model. Fig. 7d shows the difference between the estimated and accurate fraction of depth-of-discharge. In the simulation, the control algorithm was tested on a highly accurate nonlinear model of the battery. Even though a simple state-of-charge estimate is made from the linear model, simulation results show the difference between the rough estimate and the exact state-of-charge does not significantly impact the system performance. It is also shown that, under this real-time control strategy, all the batteries get the same state-of-charge at the end of charging.

In order to give a quick view of the advantage of the real-time charging strategy in respect to reducing the total charging time, it is compared with proportional rate charging strategy. The simulation is run six times each at nine discrete initial states to compare the total charging time with these two strategies. Fig. 8 shows the plots of the total charging time against the average state-of-charge of three batteries under equal rate charging strategy and real-time charging strategy for different initial battery states: (1) with real-time charging strategy and a maximum initial state-of-charge difference of 20%; (2) with real-time charging strategy and a maximum

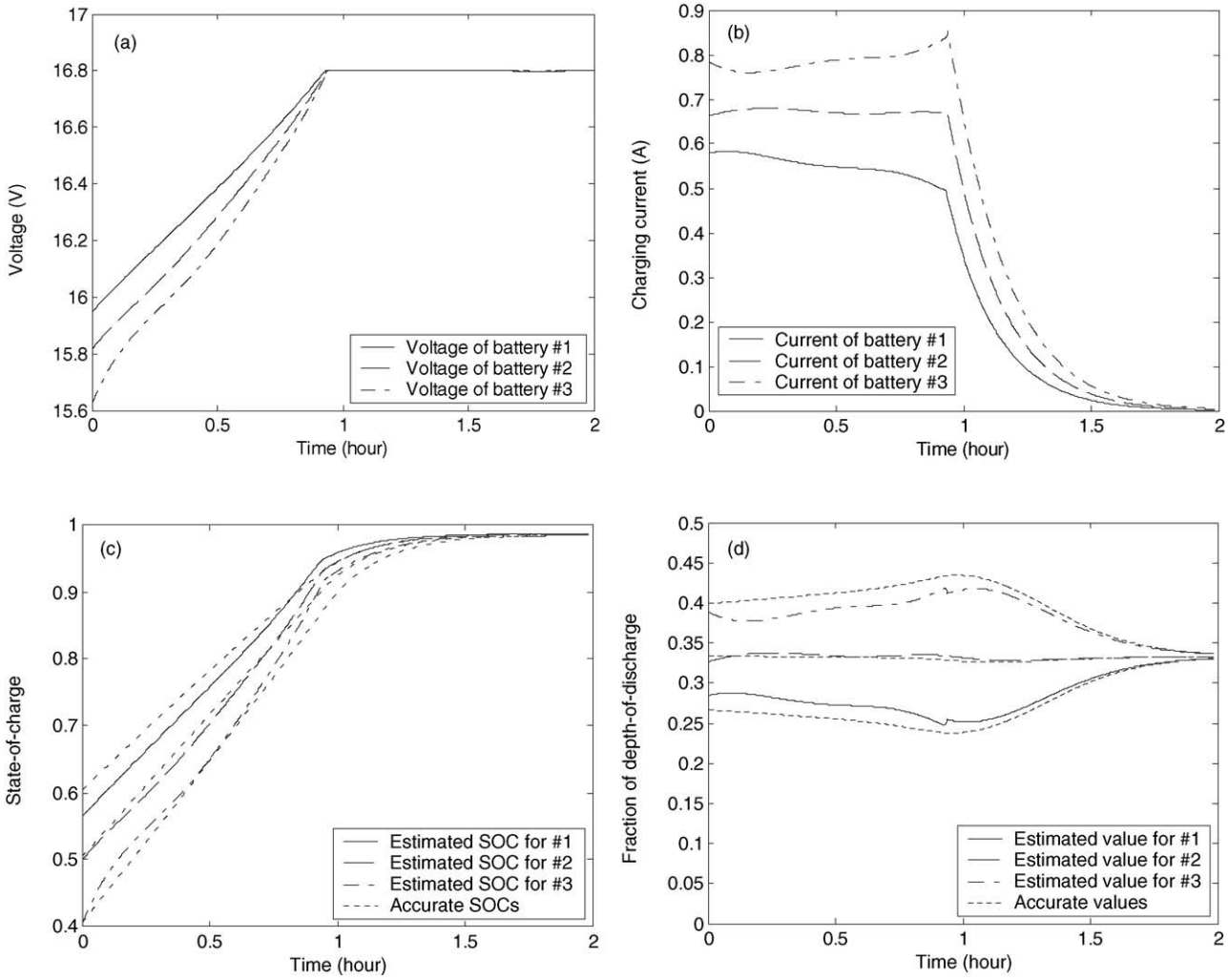

Fig. 7. Simulation results under the real-time charging strategy. (a) Voltages of the batteries, (b) charging currents of the batteries, (c) estimated and accurate states-of-charge of the batteries, (d) estimated and accurate fraction of depth-of-discharge of the batteries.

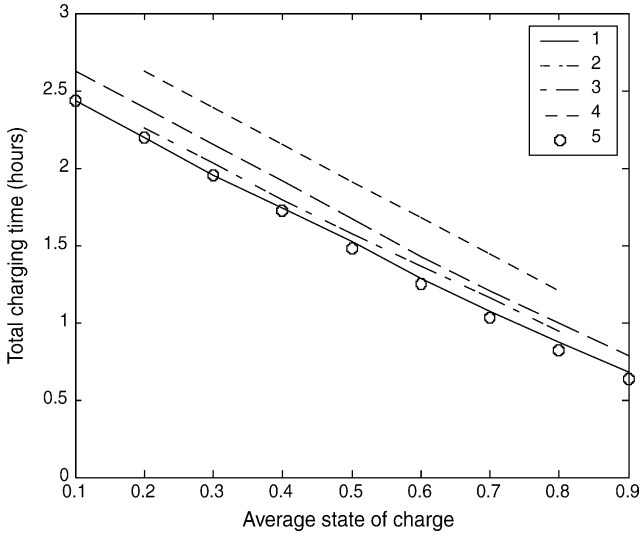

Fig. 8. Plots of the total charging time against the average state-of-charge of three batteries with equal rate charging strategy and real-time charging strategy under different initial battery states.

initial state-of-charge difference of 40%; (3) with equal rate charging strategy and a maximum initial state-of-charge difference of 20%; (4) with equal rate charging strategy and a maximum initial state-of-charge difference of 40%; (5) with either of the charging strategies and the same initial state-of-charge. The states-of-charge of the three batteries have equal difference and the average state-of-charge is their algebraic mean value. It is seen from Fig. 6 that the total charging time decreases with the average state-of-charge in spite of the control strategy or initial states of the batteries. For every initial average state-of-charge, the total charging time with real-time charging strategy is shorter than that with equal rate charging strategy. The total charging time increases with the difference in the initial state-of-charge with both strategies. The reason for real-time charging strategy is that the error of the state-of-charge estimate is bigger when their differences increase. For equal rate charging strategy, this is because it takes a longer time to charge the most depleted battery when the difference is bigger. When all batteries have the identical initial state-of-charge, both strategies have the same

effect on the current sharing and the total charging time is identical.

6. Experimental validation

Simulation results showed that the real-time control strategy provided a good coordination for the active power sharing. Next, it was validated with real hardware. A prototype of the fuel cell powered battery charging station was built using an H-Power D35 PEM fuel cell stack as the power source. This stack had a nominal power capacity of 35 W and nominal 24 V open-circuit voltage. Three 4-cell Panasonic lithium ion batteries were used. The nominal capacity of each battery was 1500 mAh. Three-buck converters were built on one single board to distribute the charging current. The block diagram of the experiment environment is shown in Fig. 9. The charging algorithm implementing the real-time control strategy resides on a general-purpose dSPACE real-time controller board, which also houses the hardware interface consisting of multi-channel analog–digital (A/D) and digital–analog (D/A) converters. The charging control algorithms are designed and implemented using Matlab/Simulink and the codes are then compiled and dropped onto a dSPACE controller board (DS1103 PPC) to control the real hardware. The charging currents and battery voltages are monitored and input to the dSPACE controller board through the A/D converters mounted on it. The power source bus voltage is also an input variable for monitoring purpose. The real-time controller provides the switch duty commands to each buck converter. The circuit protection function is also implemented within the software. This charge controller has a capability of over-voltage/over-current protection. Whenever the monitoring battery voltage is higher than a preset value (or high voltage disconnection setpoint), the controller can output a signal to turn off the corresponding charging channel. A hysteresis allows reconnecting the battery when its voltage decreases to an acceptable level. Although the reference charging current from supervisory controller module is limited to less than 1 A for each battery, this protection module can also give a shutdown signal to the power converter if the measured charging current ever exceeds this setpoint. When the total current from the fuel cell exceeds the maximum allowable value, this module output a signal to each channel to shut down all charging channels.

The experimental test was conducted with a charging algorithm implementing the real-time power sharing strategy. In order to ensure that each charging current would never exceed the safe maximum charging current (that was 800 mA for the batteries used in the experiment), the total charging current was scaled down to 1 A. The initial open-circuit voltages of the batteries were 16.2 V, 16.3 V, and 16.5 V, respectively. According to the estimated states-of-charge of the batteries, the controller would change the charging currents. The measured battery voltages and charging currents are shown in Fig. 10, where the simulated voltages and currents under the same initial conditions are also plotted. The ripples in the currents and voltage were very small. Small differences in the voltages between simulation results and experiment data were observed and this was due to the fact that more detailed transients were

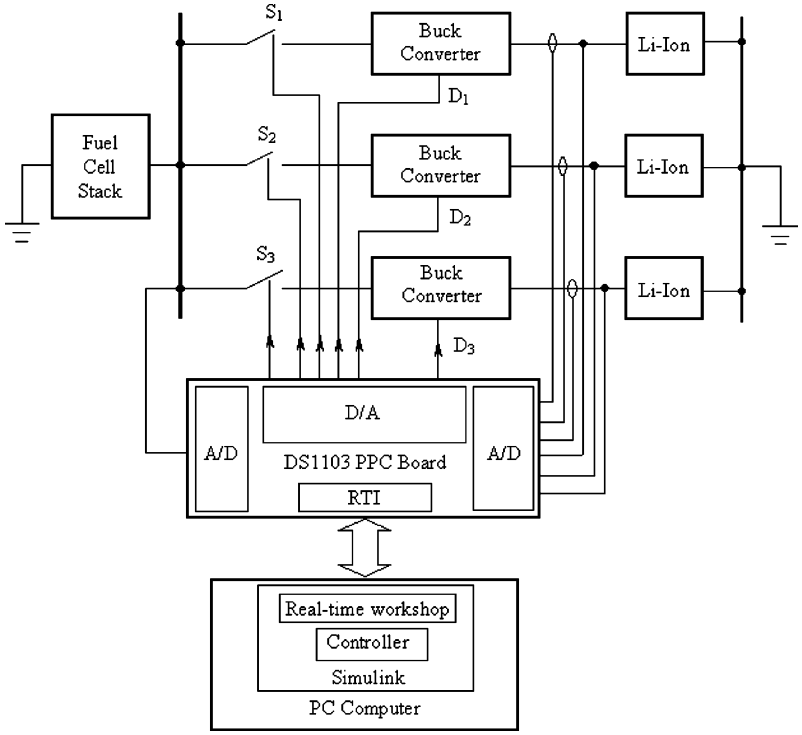

Fig. 9. Block diagram for the experiment setup.

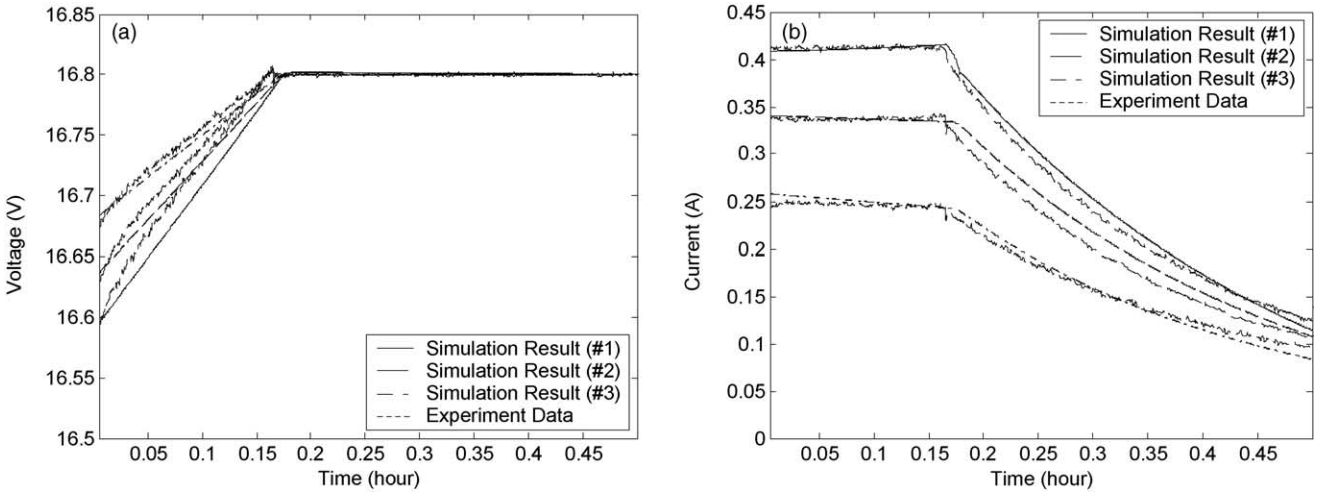

Fig. 10. The measured battery voltages and charging currents: (a) voltages, (b) currents. (a) From top to down (on the left vertical axis): voltages of batteries #3, #2, #1 (b) from top to down: charging currents for batteries #1, #2, and #3.

not characterized in the battery model. Although then, it can be said that the simulation results matched experiment data very well.

From Fig. 10, it is seen that during current regulation mode the battery voltages were different and the charging currents varied with the voltage in real-time. The battery with the lowest initial voltage (and thus the least initial charge) was charged with the highest current, and its voltage increased more rapidly than the others. This was also predicted by the simulation. This feature implies that real-time charging strategy can help to reduce the total charging time. The voltages of these batteries reached the reference voltage almost simultaneously and then their currents tapered. It is shown that all of three batteries became fully charged almost simultaneously. From the experiment results, it is also seen that the proposed method for battery state-of-charge estimation was effective for the active power sharing strategy.

7. Conclusion

This paper presents a real-time control strategy for active power sharing in a fuel cell powered battery charging station. The DC charging algorithm is developed to regulate the power distribution among the batteries. The charging controller is designed and implemented in Matlab/Simulink for both system simulation and experimental tests. Simulation and experiment results show that the proposed real-time control strategy for active power sharing can adjust the charging currents according to the estimate of state-of-charge in real-time. The estimate of state-of-charge is obtained by estimating the battery open-circuit voltage with current correction and linearly fitting between the open-circuit voltage and the state-of-charge. It is also seen that this method is effective for the active power sharing strategy. The batteries can become fully charged almost simultaneously under the real-time charging strategy. The total charging time is reduced with the real-time charging strategy, compared with equal-rate charging strategy. Experiment tests also validate the simulation results.

Acknowledgments

This work was supported in part by the US Army CECOM and the NRO under contract NRO-00-C-0134, and by US ONR under contract N00014-00-1-0368 and under contract N00014-00-1-0131.

References

[1] R.J. Brodd, Overview: rechargeable battery systems, Conference Record of WESCON'93, 1993, pp. 206–209.
[2] B. Rohland, J. Nitsch, H. Wendt, Hydrogen and fuel cells-the clean energy system, J. Power Sources 37 (January (1–2)) (1992) 271–277.
[3] A. Heinzel, C. Hebling, M. Müller, M. Zedda, C. Müller, Fuel cells for low power applications, J. Power Sources 105 (March (2)) (2002) 148–153.
[4] Z. Jiang, R. Dougal, Design and testing of a fuel-cell-powered battery-charging station, J. Power Sources 115 (April (2)) (2003) 148–153.
[5] M.M. Bernardi, M.W. Verbrugge, A mathematical model of the solid-polymer-electrolyte fuel cell, J. Electrochem. Soc. 139 (September (9)) (1992) 2477–2491.
[6] J. Kim, S. Lee, S. Srinivasan, Modeling of proton exchange membrane fuel cell performance with an empirical equation, J. Electrochem. Soc. 142 (August (8)) (1995) 2670–2674.
[7] L. Song, J.W. Evans, Electrochemical-thermal model of lithium polymer batteries, J. Electrochem. Soc. 147 (6) (2000) 2086–2095.

[8] J. Li, E. Murphy, J. Winnick, P.A. Kohl, The effects of pulse charging on cycling characteristics of commercial lithium-ion batteries, J. Power Sources 102 (December (1–2)) (2001) 302–309.
[9] T. Liu, D. Chen, C. Fang, Design and implementation of a battery charger with state-of-charge estimator, Int. J. Electron. 87 (2) (2000) 211–226.
[10] T. Lovett, A. Monti, E. Santi, R. Dougal, A multi-language environment for interactive simulation and development of controls for power electronics, in: Proceedings of IEEE 32nd Annual Power Electronics Specialists Conference, vol. 3, 2001, pp. 1725–1729.